Optimized Multimodal Nanoplatform for targeting $\alpha_v\beta_3$ integrins

Julie Bolley[a], Yoann Lalatonne[a,b], Oualid Haddad[c], Didier Letourneur[c], Michael Soussan[b],Joelle Pérard-Viret[d], Laurence Motte[a]

[a] *Université Paris 13, Sorbonne Paris Cité, Laboratoire CSPBAT, CNRS (UMR 7244) 74 avenue M. Cachin 93017 Bobigny,,France. Fax: +33 1 41 08 85 28; E-mail: Laurence.motte@univ-paris13.fr*
[b] *Department of Nuclear Medecine, Avicenne Hospital, Université Paris 13, Sorbonne Paris Cité, 74 avenue M. Cachin 93017 Bobigny,,France*
[c] *INSERM U698, 46, rue Henri Huchard 75877 Paris Cedex 18, France*
[d] *Université Paris Descartes, Sorbonne Paris Cité, Faculté de Pharmacie, CNRS (UMR 8638), 4 avenue de l'observatoire 75240 Paris cedex 06, France.*

Supporting Information

TEM image and Size distribution of γFe_2O_3@CA nanoplatform

Nanoparticles were prepared in direct micelles by oxidation of iron (II) in basic medium. γFe_2O_3@CA NPs were first prepared by mixing, for 2 hours, NPs and an excess of CA (5000 equivalents) in water at room temperature and pH 10. Residual CA was removed from the brown solid product by repeated washes with water at pH 2. The resulting γFe_2O_3@CA NPs were dispersed in distilled water at pH 7. The TEM image and the size distribution, Figure S1, show that the nanoparticles have a diameter of 9 nm with a size distribution σ=0.2.

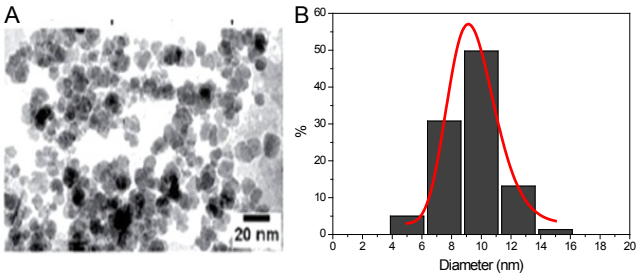

Figure S1 : TEM image (A) and size distribution (B) of γFe_2O_3@CA

Determination of CA number per nanoparticle

The average number of CA molecules was deduced using TGA, Figure S2, and following the equation 1. 1100 caffeic acids per nanoparticle were found.

$$CA/nano = \frac{n_{CA}}{n_{nano}} = \frac{m_{CA} \cdot M_{nano}}{m_{nano} \cdot M_{CA}} = \frac{\Delta m(\%) \cdot M_{nano}}{(1 - \Delta m(\%) - \Delta m_{eau}(\%)) \cdot M_{CA}} \quad \text{equation 1}$$

$$M_{nano} = \rho_{nano} \cdot V_{nano} \cdot N_A = \rho_{nano} \cdot \frac{4}{3} \cdot \pi \cdot R^3 \cdot N_A$$

$$\rho_{nano} = 5.2 \cdot 10^6 \, g \cdot m^{-3}$$
$$R = 4.5 nm$$
$$N_A = 6.022 \cdot 10^{23} \, mol^{-1}$$

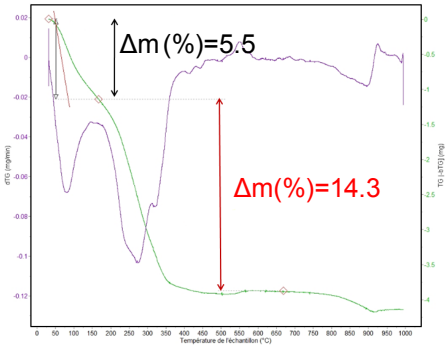

Figure S2 : TGA of γFe_2O_3@CA : loss in mass (green) and derivated (purple) curves

Magnetic measurement of γFe_2O_3@CA nanoplatform

It has to be noticed that 11 months after synthesis no decomposition of the iron oxide NPs and consequently alteration of the magnetic properties has been observed (see fig. S3).

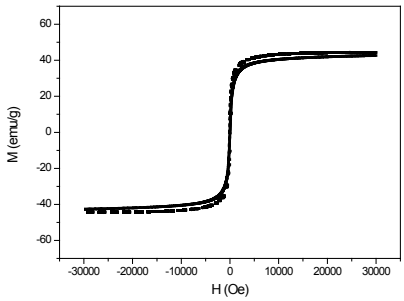

Figure S3: Magnetization as a function of the applied magnetic field curves for freshly prepared nanoparticles (full line) and 11 months old solution aging at room temperature (dot line)

Dye R123 coupling

Effect of microwaves on coupling

The efficiency of coupling at room temperature and under microwaves was studied. In the following procedures, the coupling of the dye onto the caffeic acid functionalized maghemite was performed in water in a two step procedure (activation and conjugation) at room temperature or assisted by microwaves. The microwave treatment conditions have been defined to t_{max}=3 min and T_{max}=150 °C. Several molar ratios for the R123 versus COOH functions were tested ($R = n_{R123}/n_{COOH}$). The average number of rhodamine per nanoparticle, quenching factor and yield coupling are reported in Table S1 and deduced from the calibration curve, Figure S4. These values are calculated after a 24 h treatment of γFe_2O_3@CA-R123 ferrofluid in an alkaline medium. Increasing ratio R allows higher average number of R123 per nanoparticle. For a same ratio R, using microwaves allowed to increase the average number of R123 per nanoparticle.

		Grafted Molecule Number					
	R	Before and After desorption		Quenching	%	D_h (nm)	Zeta (mV)
R123	2 RT	0	3 ± 1	5	0.3 ± 0.1	16.5	-45
	2	3 ± 1	11 ± 3	4	1 ± 0.3	24.2	-44
	20 RT	2 ±1	12 ± 1	6	1 ± 0.1	20.7	-41
	20	11 ± 1	55 ± 1	5	5 ± 0.1	32.2	-41

Table S1 : R123 number before and after molecule desorption, quenching and percentage of R123 per nanoparticle for R=2 and R=20 at room temperature (RT) or under microwaves, and dynamic light scattering properties (hydrodynamic size, polydispersity index, and zeta potential)

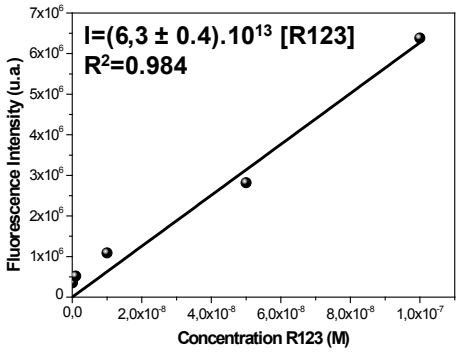

Figure S4 : Calibration curve of R123 – Evolution of the fluorescence intensity in function of R123

Study of the superparamagnetic measurement after R123 coupling

Coupling R123 on nanoparticles with a ratio R=2 or R= 20 has no impact on the superparamagnetic behavior as shown in Figure S5.

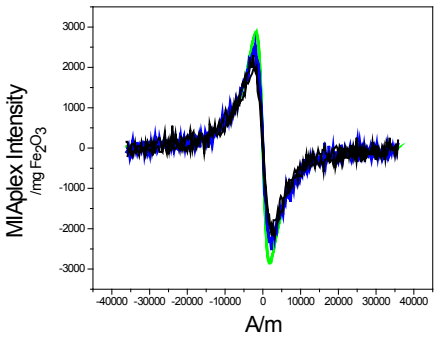

Figure S5: MIAplex® measurements on γFe_2O_3@CA (green), γFe_2O_3@CA-R123 R=2 (blue) and R=20 (black)

NH_2-PEG-COOH coupling

Determination of NH_2-PEG-COOH number by OPA method

The OPA method consists in the formation of a fluorescent product after reaction with primary amine. 50 µL of the sample was diluted in 50µL of NaOH 2N and let all night at 60°C. 1 mL of OPA reagent was added to the mixture and fluorescence measurement was recorded. In order to quantify the number of molecules per nanoparticle, a calibration curve was established and presented in Figure S6.

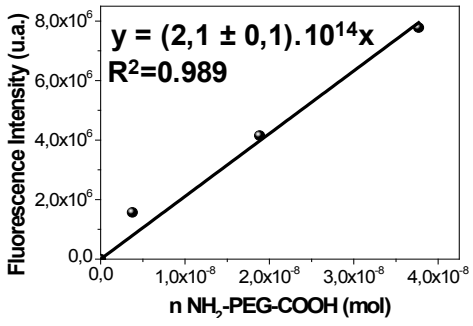

Figure S6 : Calibration curve for the determination of NH_2-PEG-COOH number by OPA method

Determination of NH_2-PEG-COOH number by TGA method

The number of NH_2-PEG-COOH on γFe_2O_3@CA for R=5 was determined by TGA and compared to the result obtained with OPA method. Compared to the nanoplatform γFe_2O_3@CA, Figure S1, a loss in mass of 1.7% is attributed to the NH_2-PEG-COOH, Figure S7. Then a number of 100 NH_2-PEG-COOH per nanoparticle is deduced using equation 1.

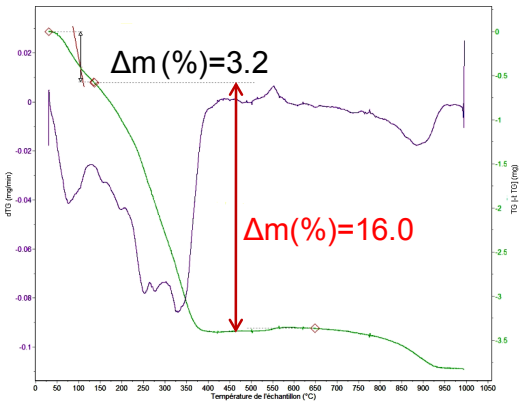

Figure S7: TGA of γFe_2O_3@CA-PEG-COOH : loss in mass (green) and derivated (purple) curves

cRGD derivatives coupling

Infra Red spectra of cRGDfK

The effect of the microwaves on cRGDfK was studied by infrared spectroscopy. The microwave treatment conditions have been defined to 3 cycles of t_{max} = 3 min and T_{max} = 65 °C. No difference was observed on infrared spectrum after microwaves irradiation, suggesting that the molecule in not deteriorated, Figure S8.

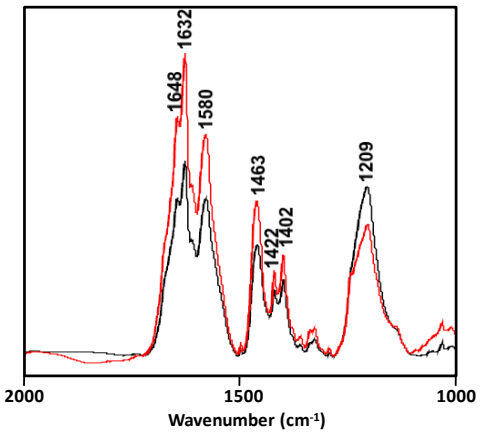

Figure S8: Infrared spectra (liquid sample) of cRGDfK before (black) and after (red) microwaves

Determination of cRGD number by Infrared Spectroscopy

Infrared spectroscopy in KBr pellets was used to qualitatively characterize the efficiency of the coupling of cRGDfK on γFe_2O_3@CA nanoplatform. However, compared to γFe_2O_3@CA nanoplatform, the infrared spectra after RGD coupling show no evidence of an efficient conjugation, Figure S9. This is attributed to the low number of cRGDfK peptides grafted on the nanoplatform.

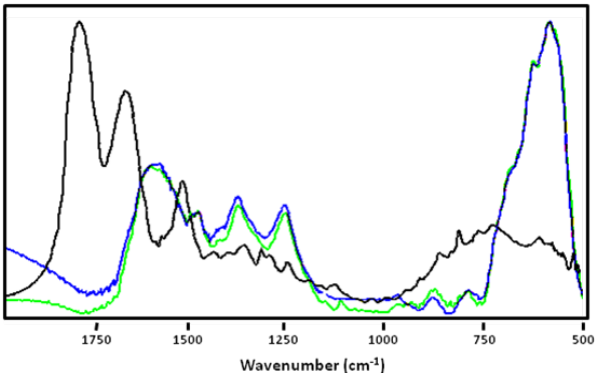

Figure S9: Infrared spectra in KBr pellets of cRGDfK (black) , γFe_2O_3@CA (green) and γFe_2O_3@CA-cRGDfK R=2 (blue)

Determination of cRGD number by OPA method

In order to quantify the number of cRGD derivatives, the OPA method is used. Calibration curves for cRGDfK and cRGDfK-PEG-NH_2 were established and presented in Figure S10.

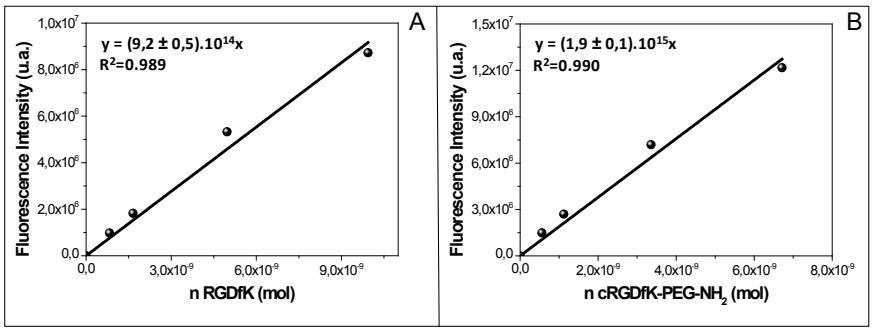

Figure S10: Calibration curves for the determination of (A) cRGDfK (R2=) and (B) cRGDfK-PEG-NH_2 *(R^2=0.990)* number by OPA method

Biological Stability

The biological stability in biological medium of the nanoplatform γFe_2O_3@CA-Dye (R=2) was studied in water, in 10% and 50% of FBS serum. The impact of the medium on quenching process is evaluated by mixing, 5µL of a γFe_2O_3@CA solution (C_{Fe}=0.04 M) with 14 µL of a R123 solution (10^{-5}M) in 1mL of medium (corresponding to R=2) and measuring the fluorescence intensity. The quenching in water, in 10% and 50% of FBS serum were similar, Table S2.

Medium	Quenching
Water	4.8
10 % serum	4.9
50% serum	4.0

Table S2 : Quenching evaluation in water, 10% and 50% of FBS serum

MRI analysis

The relaxation times were measured on a 1.5T clinical MR scanner at room temperature for various iron concentrations. Figure S10 shows the linear increases of relaxation rates with iron concentration of γFe_2O_3@CA nanoparticles and the relaxivities (r1 and r2) are deduced from the slope of the curves and are 9(±2) and 233(±7) $mM^{-1}.s^{-1}$ respectively, Figure S11.

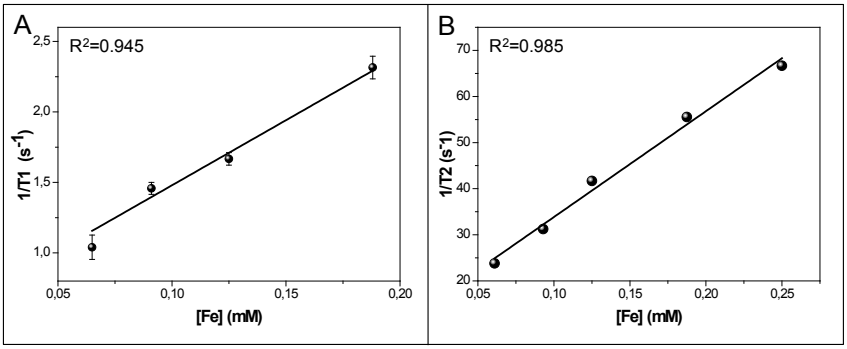

Figure S11 : Plot of (A) 1/T1 and (B) 1/T2 over Fe concentration of γFe_2O_3@CA nanoparticles

Like relaxivities r2, relaxivities r1 of the different synthesized nanoplatforms are almost constants and vary from from 9 up to 13 $mM^{-1}.s^{-1}$, depending on their functionalization, Table S3.

	r1 ($mM^{-1}.s^{-1}$)
γFe_2O_3@CA	9 ± 2
γFe_2O_3@CA-PEG-COOH R=50	9.9 ± 0.4
γFe_2O_3@CA-(PEG-cRGD) R=2	9 ± 2
Multimodal Nanoplatforms 2 steps strategy	14 ± 1
Multimodal Nanoplatforms 3 steps strategy	13 ± 2

Table S3 : Relaxivities r1 of the as-synthesized nanoplatforms

SPR analysis - Theoretical analyte binding capacity

The theoretical analyte binding capacity of a given surface is related to the amount of ligand immobilized (assuming a 1:1 binding stoichiometry), equation 2. The analyte refers to $\alpha_v\beta_3$ integrins and ligand refers to the nanoplatforms.

$$Analyte\ Binding\ Capacity\ (RU) = \frac{Analyte\ (MW)}{Ligand\ (MW)} \cdot immobilized\ Ligand\ Level\ (RU) \qquad \text{equation 2}$$

Solid Phase Binding Assay - Determination of echistatin K_d

In order to determinate the affinity constants of the nanoplatforms, the determination of the echistatin K_d is needed. Incubation of $\alpha_v\beta_3$ receptor with increasing concentrations of ^{125}I-echistatin (from 0.1 to 2.5 nM) resulted in a saturable binding, Figure S12A. Scatchard analysis of the binding data gave a linear fit with a K_d of 0.22 nM, Figure S12B.

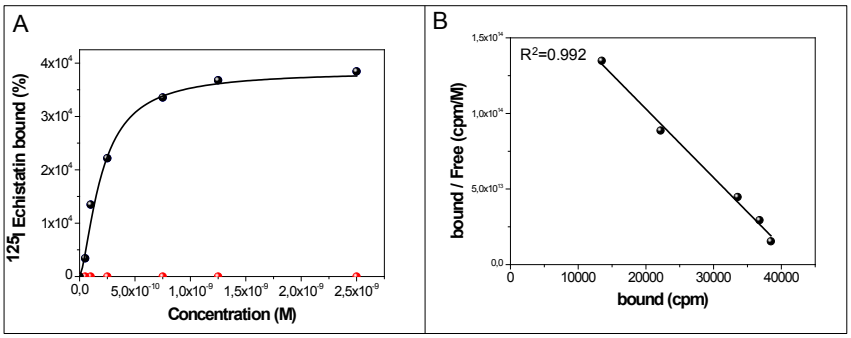

Figure S12 : (A) Saturation binding isotherm of ^{125}I-echistatin to $\alpha_v\beta_3$ and (B) determination of the ^{125}I-echistatin affinity constant from the Scatchard analysis